

Nonlinear Instability of an Electrohydrodynamic Planar Jet

Doo-Sung Lee

Department of Mathematics, College of Education, Konkuk University, 1, Hwayang-Dong, Kwangjin-Gu, Seoul, Korea

Reprint requests to Prof. D.-S. L.

Z. Naturforsch. **57a**, 682–688 (2002); received November 10, 2001

The nonlinear breakup of a fluid jet forming a plane sheet stressed at the surface by an electric field is studied. A third-order theory using the method of strained coordinates is applied to study the capillary instability of the jet. The time of breakup of the jet is obtained numerically.

Key words: Electrohydrodynamic Planar Jet; Method of Strained Coordinates; Capillary Instability.

1. Introduction

The stability of a liquid jet of circular cross-section under a small disturbance at its surface has been considered by many investigators. Work on this subject was started in the nineteenth century by Bidone, Savart, and others. Based on the linearized theory, Lord Rayleigh [1] gave a detailed analytical explanation of this phenomenon. Experimental studies [2] of the breakup of a liquid jet have shown that Rayleigh's uniform drop model is inadequate. In these experiments, nonsinusoidal deformations were observed, indicating nonlinear behavior. These observations motivated several researchers to formulate a nonlinear theory for the breakup of a liquid jets.

Yuen [3] developed a third-order nonlinear theory for this problem, using the method of straining coordinates. Wang [4], Nayfeh [5], and Lafrance [6] have also carried out nonlinear analyses of the problem. In more recent years, the electrohydrodynamic stability of capillary jets has been investigated by Gañán-Calvo [7] and Mestel [8]. All these investigations dealt with circular columnar jets. Nonlinear analyses of planar jets have received relatively little attention. The physical properties of liquid jets play a fundamental role in applications such as spray drying, electronic ink-jet printing, spinning of synthetic fibers, and fuel atomization.

In this paper, a nonlinear problem is considered in which a jet of fluid in the form of a plane sheet is stressed at the surface by fields. Although the influence of an electrical field on the surface waves of a planar jet has been studied both theoretically and experimentally by Melcher [9] and Crowley [10], their investigations were confined to a linear theory. In the present paper, by the method of straining coordinates [11], we have devel-

oped a third order nonlinear theory on the propagation of waves over the surface of a planar jet stressed by a constant electrical field.

A planar jet is difficult to produce in the laboratory, but many of the salient characteristics of the more easily produced circular jet can be understood in detail in planar geometry.

2. Basic Equations

We consider an incompressible, inviscid fluid jet in the form of a thin sheet. The configuration of the jet, stressed by an equilibrium electric field perpendicular to its surfaces, is shown in Fig. 1. The jet is assumed to be infinitely conducting and to be projected with a constant velocity U_0 . Let $2h$ be the equilibrium thickness of the fluid jet. We use Cartesian coordinates (x, z) with z axis taken along the axis of the jet. The electric field is ap-

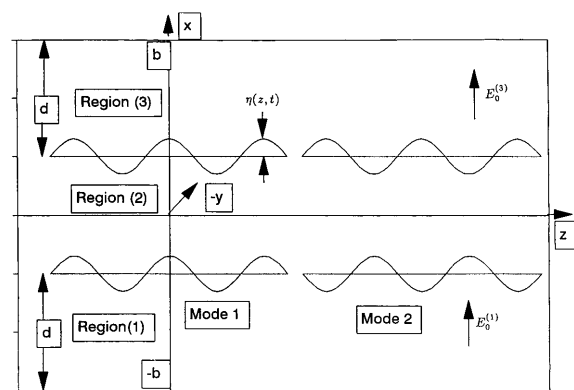


Fig. 1. Configuration of the planar jet between parallel, perfectly conducting electrodes.

plied by means of external rigid, perfectly conducting parallel electrodes at $x = \pm b$, or at a distance $\pm d$ from the interface, which is a function of z and time.

Let $\eta(z, t)$ denote the elevation of the free surface measured from the unperturbed level $x = h$. The consequential dynamics are retained if regions (1) and (3), external to the jet, are assumed to be filled with a fluid of small density (compared to the density of the fluid in the jet). Note that all modes that depend on the y coordinate, as well as the effects of gravity are ignored. Now, a periodic initial disturbance is given at the surface of the jet. The motion is assumed to be irrotational. If \mathbf{u} and \mathbf{E} denote the velocity and electric field, respectively, at any time t , then

$$\nabla \cdot \mathbf{u} = 0, \quad \nabla \cdot \mathbf{E} = 0.$$

If ϕ and ψ denote dimensionless velocity and electric potential, respectively, so that $\mathbf{u} = \nabla\phi$, and $\mathbf{E} = -\nabla\psi$, then the equations for ϕ and ψ are given by

$$(\Delta\phi) = \nabla^2\phi = 0, \quad (2.1)$$

for $-h + \eta^{(1)} \leq x \leq h + \eta^{(3)}$, and

$$(\Delta\psi) = \nabla^2\psi = 0, \quad (2.2)$$

for $b \geq x \geq h + \eta^{(3)}$ and $-b \leq x \leq -h + \eta^{(1)}$, where $\eta^{(1)}(z, t)$ and $\eta^{(3)}(z, t)$ are the elevations of the free surfaces measured from the unperturbed levels. Since there are two interfaces, we have two functions $\eta^{(1)}(z, t)$ and $\eta^{(3)}(z, t)$. The unit normal \mathbf{n} to the surface is given by

$$\mathbf{n} = \frac{\nabla F}{|\nabla F|} = -\eta_z(\eta_z^2 + 1)^{-\frac{1}{2}}\mathbf{e}_z + (\eta_z^2 + 1)^{-\frac{1}{2}}\mathbf{e}_x, \quad (2.3)$$

where $F = 0$ is the equation of the surface of jet. The condition that the electric field is satisfied on the deformed surface of the jet and at external boundaries is

$$\mathbf{n} \times [\mathbf{E}] = 0 \quad \text{at } x = h + \eta^{(3)} \text{ and } x = b, \quad (2.4)$$

where $[\cdot]$ represents the jump across the surface of the jet, and similar for region (1). (Note that equilibrium requires that $|E_0^{(3)}| = |E_0^{(1)}| = E_0$.) At the free surface, the normal stress is continuous

$$\begin{aligned} n_\alpha [p] - n_\beta [M_{\alpha\beta}] &= 0 \quad \text{at } x = h + \eta^{(3)} \\ \text{and } x &= -h + \eta^{(1)}, \end{aligned} \quad (2.5)$$

where n_α is the unit normal vector given by (2.3), and p is the pressure. The force $M_{\alpha\beta}$ can be divided into two parts, a part that has a mechanical origin and a part that has an electric origin. Thus

$$M_{\alpha\beta} = M_{\alpha\beta}^e + M_{\alpha\beta}^m,$$

where

$$M_{\alpha\beta}^e = \epsilon_0 \left(E_\alpha E_\beta - \frac{1}{2} \delta_{\alpha\beta} E_\gamma E_\gamma \right), \quad (2.6)$$

with ϵ_0 being the permittivity, and

$$[M_{\alpha\beta}^m] = \delta_{\alpha\beta} T \eta_{zz} (1 + \eta_z^2)^{-3/2}, \quad (2.7)$$

where T is the surface tension and $\delta_{\alpha\beta}$ the Kronecker delta. The pressure p can be evaluated using Bernoulli's equation. We obtain

$$p = -\frac{1}{2} \rho [\phi_x^2 + \phi_z^2] - \rho \phi_t + f(t), \quad (2.8)$$

where $f(t)$ stands for the integration constant with respect to the space variables.

All physical variables are normalized by using half of the thickness of the undisturbed jet h for the characteristic length, $\sqrt{T/\rho h}$ for the characteristic speed, and $hE_0^2\epsilon_0/T$ for the characteristic electric field parameter. Here, E_0 denotes the strength at the surface of the undeformed jet. In the following, the primes on the dimensionless variables $\eta' = \eta/h$, $b' = b/h$, $h' = d/h$, and so on, are omitted for conciseness.

The fact that the interface is moving with the fluid leads to

$$\begin{aligned} \frac{\partial \eta}{\partial t} - \frac{\partial \phi}{\partial x} &= -\frac{\partial \phi}{\partial z} \frac{\partial \eta}{\partial z} \quad \text{at } x = 1 + \eta^{(3)} \\ \text{and } x &= -1 + \eta^{(1)}. \end{aligned} \quad (2.9)$$

Now the boundary condition at the free surface is, from (2.5),

$$\begin{aligned} & -\frac{\partial \phi}{\partial t} - \frac{1}{2} \left[\left(\frac{\partial \phi}{\partial x} \right)^2 + \left(\frac{\partial \phi}{\partial z} \right)^2 \right] \\ & + \frac{\partial^2 \eta}{\partial z^2} \left[1 + \left(\frac{\partial \eta}{\partial z} \right)^2 \right]^{-3/2} \\ & + \Gamma \left[\left(-\frac{\partial \psi}{\partial z} \frac{\partial \eta}{\partial z} + \frac{\partial \psi}{\partial x} \right)^2 \left\{ 1 + \left(\frac{\partial \eta}{\partial z} \right)^2 \right\}^{-1} \right. \\ & \left. - \frac{1}{2} |\nabla \psi|^2 \right] = \frac{\Gamma}{2}, \end{aligned} \quad (2.10)$$

where

$$\Gamma = \frac{\epsilon_0 E_0^2 h}{T}.$$

Since the fluid is infinitely conducting, (2.4) can be written as

$$\begin{aligned} \frac{\partial \psi}{\partial x} \frac{\partial \eta}{\partial z} + \frac{\partial \psi}{\partial z} &= 0 \quad \text{at } x = 1 + \eta^{(3)}(z, t) \\ \text{and } x &= -1 + \eta^{(1)}(z, t), \end{aligned} \quad (2.11a)$$

and

$$\frac{\partial \psi}{\partial z} = 0 \quad \text{at } x = \pm 1. \quad (2.11b)$$

At $t = 0$, the disturbance of the amplitude η_0 and wave number k is imposed on the surface $x = \pm 1$ of the jet. We assume the initial conditions to be

$$\eta(z, 0) = \eta_0 \cos kz - 1, \quad (2.12)$$

$$\partial \eta(z, 0)/\partial t = 0. \quad (2.13)$$

The nonlinear stability problem posed by (2.1)–(2.2) and (2.9)–(2.13) is examined by the method of the strained coordinates [9]. We now assume that the surface disturbance and the potential functions can be expanded in a perturbation series in terms of the smallness parameter η_0 . Thus, we write

$$\phi(x, t) = \sum_{n=1}^{\infty} \eta_0^n \phi_n(z, t), \quad (2.14)$$

$$\psi(x, t) = \sum_{n=0}^{\infty} \eta_0^n \psi_n(z, t), \quad (2.15)$$

and

$$\eta(x, t) = \sum_{n=1}^{\infty} \eta_0^n \eta_n(z, t). \quad (2.16)$$

Now we use the strained coordinates

$$\tau = t\nu = t \left[\sum_{n=1}^{\infty} \nu_n \eta_0^{n-1} \right], \quad (2.17)$$

$$\xi = k_c z = z \left[\sum_{n=1}^{\infty} k_n \eta_0^{n-1} \right]. \quad (2.18)$$

If we substitute (2.14)–(2.16) into (2.9)–(2.11), boundary conditions of various orders are obtained. A Maclaurin series expansion of the boundary conditions at $r = 1$ provides successive orders of approximation to these conditions which are then used to specify the problem in those orders.

3. Linear Theory

We substitute the expressions (2.14), (2.15) and (2.16) for ϕ , ψ and η , respectively into the field equations (2.1) and (2.2), the boundary conditions (2.9)–(2.11), and initial conditions (2.12)–(2.13). Equating the coefficient of first power of η_0 leads to

$$\nabla_0^2 \phi_1 = 0, \quad (3.1)$$

$$\nabla_0^2 \psi_1 = 0, \quad (3.2)$$

where

$$\nabla_0^2 = \frac{\partial^2}{\partial x^2} + k_1^2 \frac{\partial^2}{\partial \xi^2}.$$

The various boundary conditions at the interface are, for the region (3) (at $x = 1$)

$$\nu_1 \frac{\partial \eta_1}{\partial \tau} - \frac{\partial \phi_1}{\partial x} = 0, \quad (3.3)$$

$$\frac{\partial \psi_1}{\partial \xi} + \frac{\partial \eta_1}{\partial \xi} \frac{\partial \psi_0}{\partial x} = 0, \quad (3.4)$$

$$-\nu_1 \frac{\partial \phi_1}{\partial \tau} + k_1^2 \frac{\partial^2 \eta_1}{\partial \xi^2} + \Gamma \frac{\partial \psi_1}{\partial x} \frac{\partial \psi_0}{\partial x} = 0, \quad (3.5)$$

where

$$\frac{\partial \psi_0}{\partial x} = -1. \quad (3.6)$$

At $x = b$, from the boundary condition (2.11b), we have

$$\frac{\partial \psi_1}{\partial \xi} = 0. \quad (3.7)$$

The initial conditions are

$$\eta^{(1)}(\xi, 0) = \cos \mathcal{H} \xi, \quad (3.8)$$

$$\begin{aligned} \partial \eta^{(1)}(\xi, 0)/\partial \tau &= \partial \eta^{(3)}(\xi, 0)/\partial \tau = 0, \\ \eta^{(1)}(\xi, 0) &= \eta^{(3)}(\xi, 0), \end{aligned} \quad (3.9)$$

where the wave number \mathcal{H} in the strained coordinate system has the representation $\mathcal{H} = k/k_c$. For the first order solutions we set $\nu_1 = 1$. The solutions (mode 1 (sinuous)) are identical to linearized analysis and are as follows:

$$\eta_1^{(3)}(\xi, \tau) = \cosh \omega_1 \tau \cos \mathcal{H} \xi, \quad (3.10)$$

$$\phi_1 = \frac{\omega_1}{K} \frac{\sinh Kx}{\cosh K} \sinh \omega_1 \tau \cos \mathcal{H} \xi, \quad (3.11)$$

$$\psi_1^{(3)} = \frac{\sinh K(b-x)}{\sinh Kd} \cosh \omega_1 \tau \cos \mathcal{H} \xi, \quad (3.12)$$

$$\begin{aligned} \eta_1^{(1)}(\xi, \tau) &= \eta_1^{(3)}(\xi, \tau), \\ \psi_1^{(1)}(x, \xi, \tau) &= \psi_1^{(3)}(-x, \xi, \tau), \end{aligned} \quad (3.13)$$

where

$$\omega_1^2 = K^2 C_a \{ \Gamma \mathcal{C}(K) - K \}, \quad (3.14)$$

$$C_a = \coth K, \quad \mathcal{C}(K) = \coth Kd, \quad K = k_1 \mathcal{H}.$$

From (3.14) we see that, when the wave number is greater than k_1 , where k , is given by the relation

$$k_1 - \Gamma \coth(k_1 d) = 0, \quad (3.15)$$

ω_1 is pure imaginary, and the solutions are stable. When $K < k_1$, the surface wave is unstable. The variation with Γ of these values k_1 is shown in Figure 2.

The solution of another mode (mode 2 (varicose)) is obtained by virtue of the conservation of mass when the initial condition (3.9) is replaced by

$$\eta^{(1)}(\xi, 0) = -\eta^{(3)}(\xi, 0). \quad (3.16)$$

In this case the velocity potential is given as

$$\phi_1 = \frac{\omega_1}{K} \frac{\cosh Kx}{\sinh K} \sinh \omega_1 \tau \cos \mathcal{H}\xi, \quad (3.17)$$

where

$$\omega_1^2 = \frac{K^2}{C_a} \{\Gamma \mathcal{C}(K) - K\}, \quad (3.18)$$

and $\eta_1^{(3)}(\xi, \tau)$ and $\psi_1^{(3)}(x, \xi, \tau)$ are the same as (3.10) and (3.12), respectively, however

$$\begin{aligned} \eta_1^{(1)}(\xi, \tau) &= -\eta_1^{(3)}(\xi, \tau), \\ \psi_1^{(1)}(x, \xi, \tau) &= -\psi_1^{(3)}(-x, \xi, \tau). \end{aligned} \quad (3.19)$$

Equations (3.14) and (3.18) agree with those given by Melcher [7, p. 80]. In the following we give mode 2 solutions.

4. Second Order Solutions

We now proceed to the second order problem in $O(\eta_0^2)$. We have to solve the equations

$$\nabla_0^2 \phi_2 = -2k_1 k_2 \frac{\partial^2 \phi_1}{\partial \xi^2}, \quad (4.1)$$

$$\nabla_0^2 \psi_2 = -2k_1 k_2 \frac{\partial^2 \psi_1}{\partial \xi^2}, \quad (4.2)$$

subjected to the following boundary conditions at $x = 1$:

$$\begin{aligned} -v_1 \frac{\partial \eta_2}{\partial \tau} + \frac{\partial \phi_2}{\partial x} \\ = -\frac{1}{2} \omega_1 K C_a \sinh 2\omega_1 \tau \cos 2\mathcal{H}\xi, \end{aligned} \quad (4.3)$$

$$\begin{aligned} \frac{\partial \psi_2}{\partial \xi} + \frac{\partial \eta_2}{\partial \xi} \frac{\partial \psi_0}{\partial x} \\ = -\frac{1}{2} K^2 \mathcal{C}(K) (1 + \cosh 2\omega_1 \tau) \sin 2\mathcal{H}\xi, \end{aligned} \quad (4.4)$$

$$\begin{aligned} -v_1 \frac{\partial \phi_2}{\partial \tau} + k_1^2 \frac{\partial^2 \eta_2}{\partial \xi^2} + \Gamma \frac{\partial \psi_2}{\partial x} \frac{\partial \psi_0}{\partial x} \\ = \frac{1}{8} [\omega_1^2 (1 - C_a^2) - \Gamma K^2 (\mathcal{C}^2(K) - 1) \\ + \cosh 2\omega_1 \tau \{\omega_1^2 (3 + C_a^2) - \Gamma K^2 (\mathcal{C}^2(K) - 1)\}] \\ + \frac{1}{8} \cos 2\mathcal{H}\xi [\omega_1^2 (1 + C_a^2) \\ - \Gamma K^2 (\mathcal{C}^2(K) - 3) + \cosh 2\omega_1 \tau \\ \cdot \{\omega_1^2 (3 - C_a^2) - \Gamma K^2 (\mathcal{C}^2(K) - 3)\}], \end{aligned} \quad (4.5)$$

where we have set both v_2 and k_2 equal to zero, and at $x = b$ we have

$$\frac{\partial \psi_2}{\partial \xi} = 0, \quad (4.6)$$

and the initial data for the second order problem are

$$\eta_2(\xi, 0) = 0, \quad \partial \eta_2 / \partial \tau = 0. \quad (4.7)$$

Since it is cumbersome to put superscript 3 on every ψ and η we omit it for convenience. For the solution of the second order problem we assume

$$\eta_2(\xi, \tau) = B_{22}(\tau) \cos 2\mathcal{H}\xi. \quad (4.8)$$

Using (4.8) and first order solutions in (4.1)–(4.7), we obtain the following second order solutions:

$$B_{22}(\tau) = a_{22} \cosh \omega_2 \tau + b_{22} \cosh 2\omega_1 \tau + c_{22}, \quad (4.9)$$

$$\psi_2(\tau) = \Psi_{22}(\tau) \frac{\sinh(2K(b-x))}{\sinh 2Kd} \cos 2\mathcal{H}\xi, \quad (4.10)$$

$$\begin{aligned} \phi_2(\tau) = \left[\frac{\partial B_{22}(\tau)}{\partial \tau} + P_{22} \sinh 2\omega_1 \tau \right] \\ \cdot \frac{\cosh 2Kx}{2K \sinh 2K} \cos 2\mathcal{H}\xi + F(\tau), \end{aligned} \quad (4.11)$$

where

$$a_{22} = -(b_{22} + c_{22}), \quad (4.12)$$

$$\begin{aligned} b_{22} = \frac{K}{4C_b(\omega_2^2 - 4\omega_1^2)} \\ \cdot [\omega_1^2 (3 - C_a^2) - 4\omega_1^2 C_a C_b - \Gamma \Delta], \end{aligned} \quad (4.13)$$

$$c_{22} = \frac{K}{4C_b \omega_2^2} [\omega_1^2 (1 + C_a^2) - \Gamma \Delta], \quad (4.14)$$

$$\Delta = K^2 \{4\mathcal{C}(2K)\mathcal{C}(K) + \mathcal{C}^2(K) - 3\}, \quad (4.15)$$

$$\begin{aligned} \Psi_{22} = a_{22} \cosh \omega_2 \tau \\ + (b_{22} + S_{22}) \cosh 2\omega_1 \tau + c_{22} + S_{22}, \end{aligned} \quad (4.16)$$

$$S_{22} = \frac{1}{4} K \mathcal{C}(K), \quad P_{22} = -\frac{1}{2} \omega_1 K C_a, \quad (4.17)$$

$$F(\tau) = -\frac{\tau}{8} [\omega_1^2 (1 - C_a^2) - \Gamma K^2 (\mathcal{C}^2(K) - 1)] \\ - \frac{1}{16 \omega_1} \sinh 2 \omega_1 \tau \\ \cdot [\omega_1^2 (3 + C_a^2) - \Gamma K^2 (\mathcal{C}^2(K) - 1)], \quad (4.18)$$

and

$$\omega_2^2 = \frac{4 K^2}{C_b} \{\Gamma \mathcal{C}(2K) - 2K\}, \quad (4.19)$$

with

$$C_b = \coth 2K, \quad \mathcal{C}(2k) = \coth 2Kd. \quad (4.20)$$

The solution for the region 1 is similar.

5. Third Order Problem

We use the first and second order solutions to derive the solution of the third order problem

$$\nabla_0^2 \phi_3 = 2k_1 k_3 \mathcal{H}^2 \omega_1 \frac{\cosh Kx}{K \sinh K} \sinh \omega_1 \tau \cos \mathcal{H} \xi, \quad (5.1)$$

$$\nabla_0^2 \psi_3 = 2k_1 k_3 \mathcal{H}^2 \frac{\sinh(K(b-x))}{\sinh Kd} \\ \cdot \cosh \omega_1 \tau \cos \mathcal{H} \xi. \quad (5.2)$$

The boundary conditions at $x = 1$ are as follows:

$$-\frac{\partial \eta_3}{\partial \tau} + \frac{\partial \phi_3}{\partial x} = P_{31}(\tau) \cos \mathcal{H} \xi \\ + P_{33}(\tau) \cos 3\mathcal{H} \xi, \quad (5.3)$$

$$\psi_3 + \eta_3 \frac{\partial \psi_0}{\partial x} = R_{31}(\tau) \cos \mathcal{H} \xi \\ + R_{33}(\tau) \cos 3\mathcal{H} \xi, \quad (5.4)$$

$$-\frac{\partial \phi_3}{\partial \tau} + k_1^2 \frac{\partial^2 \eta_3}{\partial \xi^2} + \Gamma \frac{\partial \psi_3}{\partial x} \frac{\partial \psi_0}{\partial x} \\ = [Q_{31}(\tau) - \Gamma S_{31}(\tau)] \cos \mathcal{H} \xi \\ + [Q_{33}(\tau) - \Gamma S_{33}(\tau)] \cos 3\mathcal{H} \xi, \quad (5.5)$$

and $\psi_3(b, \xi, \tau) = 0$, and the initial conditions are

$$\eta_3(\xi, 0) = 0, \quad \partial \eta_3(\xi, 0) / \partial \tau = 0. \quad (5.6)$$

The complete expressions for the right-hand sides of (4.3), (4.4), (4.5), (5.3), (5.4), and (5.5), as well as for P , Q , R and S can be obtained, on request from the author. Following the same approach as in Sect. 4, we assume

$$\eta_3(\tau) = B_{31}(\tau) \cos \mathcal{H} \xi + B_{33}(\tau) \cos 3\mathcal{H} \xi. \quad (5.7)$$

The third order electric and velocity potentials are now

$$\psi_3 = \left[(B_{31}(\tau) + R_{31}(\tau)) \frac{\sinh(K(b-x))}{\sinh Kd} \right. \\ - k_3 \mathcal{H} d \mathcal{C}(K) \frac{\sinh(K(b-x))}{\sinh Kd} \cosh \omega_1 \tau \\ + k_3 \mathcal{H}(b-x) \frac{\cosh(K(b-x))}{\sinh Kd} \cosh \omega_1 \tau \left. \right] \cos \mathcal{H} \xi \\ + \{B_{33}(\tau) + R_{33}(\tau)\} \frac{\sinh(3K(b-x))}{\sinh 3Kd} \cos 3\mathcal{H} \xi, \quad (5.8)$$

$$\phi_3 = \left[\left\{ \frac{\partial B_{31}(\tau)}{\partial \tau} + P_{31}(\tau) - k_3 \omega_1 \mathcal{H} \sinh \omega_1 \tau \right\} \right. \\ \cdot \frac{\cosh Kx}{K^2 \sinh K} + k_3 \omega_1 \mathcal{H} \frac{(x-1) \sinh Kx}{K \sinh K} \sinh \omega_1 \tau \left. \right] \\ \cdot \cos \mathcal{H} \xi + \left\{ \frac{\partial B_{33}(\tau)}{\partial \tau} + P_{33}(\tau) \right\} \\ \cdot \frac{\cosh 3Kx}{3K \sinh 3K} \cos 3\mathcal{H} \xi. \quad (5.9)$$

Substituting from (5.8) and (5.9) into (5.5), from the coefficients of $\cos \mathcal{H} \xi$ we obtain the following differential equation to determine $B_{31}(\tau)$:

$$\frac{\partial^2 B_{31}(\tau)}{\partial \tau^2} - \omega_1^2 B_{31}(\tau) \\ = - \left[\mu_1 p_{311} + \frac{K}{C_a} \right. \\ \cdot \{q_{311} - \Gamma(S_{311} + K \mathcal{C}(K) R_{311})\} \left. \right] \cosh \mu_1 \tau \\ - \left[\mu_2 p_{312} + \frac{K}{C_a} \right. \\ \cdot \{q_{312} - \Gamma(S_{312} + K \mathcal{C}(K) R_{312})\} \left. \right] \cosh \mu_2 \tau \\ - \left[3\omega_1 p_{313} + \frac{K}{C_a} \right. \\ \cdot \{q_{313} - \Gamma(S_{313} + K \mathcal{C}(K) R_{313})\} \left. \right] \cosh 3\omega_1 \tau \\ - \left[\omega_1 p_{314} + \frac{K}{C_a} \right. \\ \cdot \{q_{314} - \Gamma(S_{314} + K \mathcal{C}(K) R_{314})\} \\ - \frac{k_3}{k_1} \left\{ \omega_1^2 - \Gamma \frac{K^2}{C_a} (Kd \mathcal{C}^2(K) - \mathcal{C}(K) - Kd) \right\} \left. \right] \\ \cdot \cosh \omega_1 \tau. \quad (5.10)$$

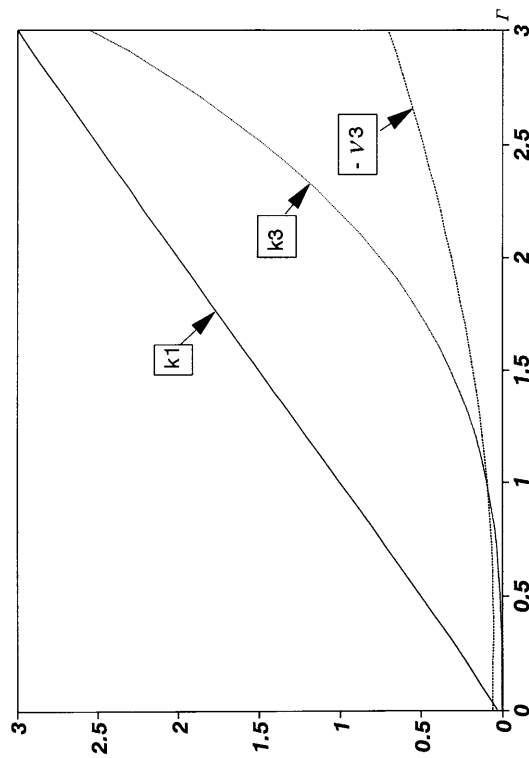


Fig. 2. The variation with Γ of the linear cutoff wave numbers k_1 and k_3 , and $-v_3$ ($d = 10$).

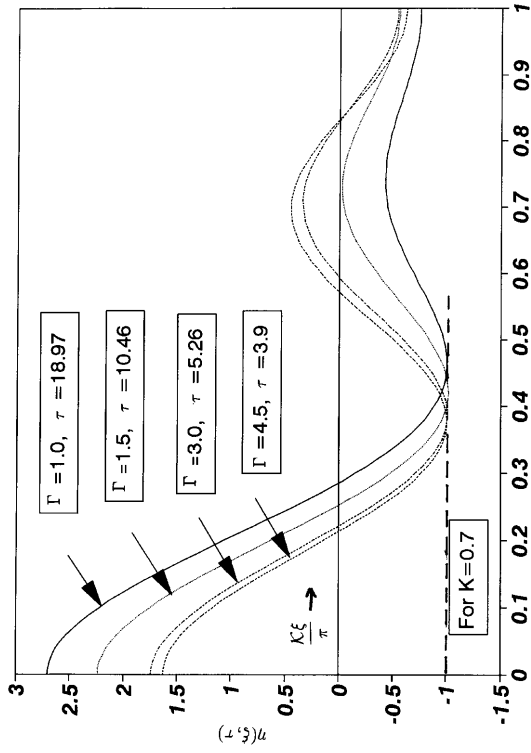


Fig. 3. Wave profiles at the breakup for the dimensionless wave number ($d = 10$, $\eta_0 = 0.01$).

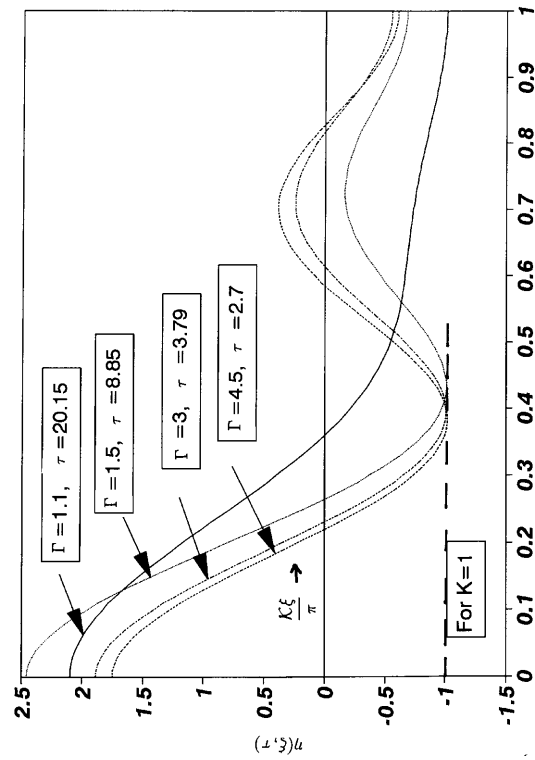


Fig. 4. Wave profiles at the breakup for the dimensionless wave number ($d = 10$, $\eta_0 = 0.01$).

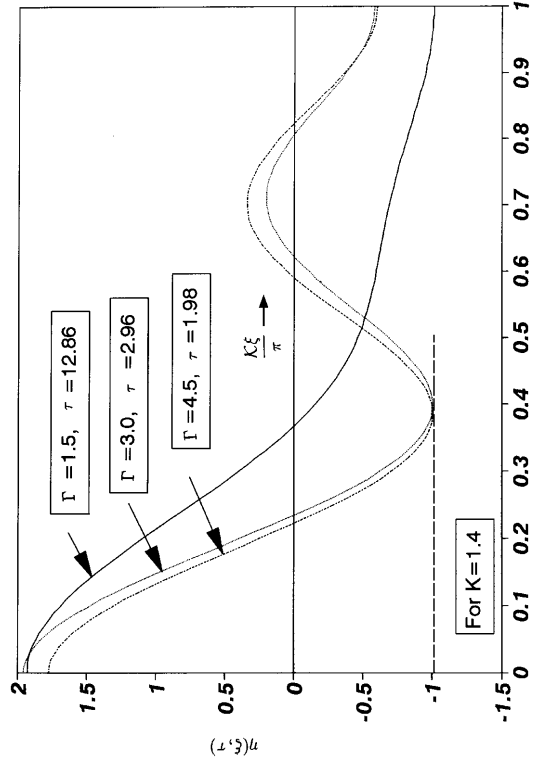


Fig. 5. Wave profiles at the breakup for the dimensionless wave number ($d = 10$, $\eta_0 = 0.01$).

In order η_3 to be stable for $K > k_1$, the last term (5.10) has to be set equal to be zero. This determines v_3 , which can be shown to be

$$\begin{aligned} v_3 = & \frac{1}{8} \gamma K C_a - \frac{1}{8} \alpha \frac{K}{C_a} \\ & - \frac{1}{8} \beta \left(-2 K C_b + \frac{K}{C_a} \right) + \frac{k_3}{2 k_1} \\ & + \Gamma \frac{K^2}{2 C_a} G(K) \\ & \cdot \{ A(3 - C_a^2 - 4 C_a C_b) + 2 B(1 + C_a^2) \} \\ & + \frac{K}{C_a \omega_1^2} \left[\frac{9 K^4}{64} - K^2 \frac{k_3}{k_1} + \frac{\Gamma}{2} \right. \\ & \cdot \left. \left\{ -K(A + 2 B) G(K) \Gamma \Delta + H(K) \right. \right. \\ & \left. \left. - \frac{k_3}{k_1} K(K d \mathcal{C}^2(K) - \mathcal{C}(K) - K d) \right\} \right], \quad (5.11) \end{aligned}$$

$$A = \frac{1}{4 C_b (\omega_2^2 - 4 \omega_1^2)}, \quad B = \frac{1}{4 C_b \omega_2^2}, \quad (5.12)$$

$$G(K) = K^2 [\mathcal{C}(K) \{4 \mathcal{C}(2K) + \mathcal{C}(K)\} - 3]/4, \quad (5.13)$$

$$H(K) = 3 K^3 \mathcal{C}(K) \{2 \mathcal{C}(2K) \mathcal{C}(K)\} - 3/8, \quad (5.14)$$

Equation (5.11) shows that v_3 is infinite when $\omega_1 = 0$ at $K = k_1$. Thus, for v_3 to be finite at $\omega_1 = 0$, we equate to zero the quantity in the bracket of the last term of (5.11) when $K = k_1$. Thus

$$k_3 = \frac{9 k_1^4 + 32 \Gamma \{H(k_1) - 3 k_1 G(k_1) \Gamma \Delta / 4 C_b \omega_2^2\}}{64 \{k_1 + \Gamma (k_1 d \mathcal{C}^2(k_1) - \mathcal{C}(k_1) - k_1 d) / 2\}}. \quad (5.15)$$

The differential equation for $B_{33}(\tau)$ is analogously obtained by equating the coefficients of $\cos 3\mathcal{H}\xi$ in (5.5). Solutions of these differential equations furnish $B_{31}(\tau)$ and $B_{33}(\tau)$ as

$$\begin{aligned} B_{31}(\tau) = & a_{31} \cosh \omega_1 \tau \\ & + b_{31} \cosh \omega_1 \tau \cosh \omega_2 \tau \\ & + c_{31} \sinh \omega_1 \tau \sinh \omega_2 \tau + d_{31} \cosh 3 \omega_1 \tau, \quad (5.16) \end{aligned}$$

$$\begin{aligned} B_{33}(\tau) = & a_{33} \cosh \omega_3 \tau \\ & + b_{33} \cosh \omega_1 \tau \cosh \omega_2 \tau \\ & + c_{33} \sinh \omega_1 \tau \sinh \omega_2 \tau + d_{33} \cosh 3 \omega_1 \tau, \\ & + e_{33} \cosh \omega_1 \tau. \quad (5.17) \end{aligned}$$

The expressions of a_{31}, \dots , and e_{33} can be obtained, on request, from the author.

6. Numerical Results

In Fig. 2 we display the variation with Γ of the linear cutoff wave number k_1 , roots of (3.15) when $d = 10$. Also k_3 , and v_3 when $K = k_1$ in (5.11), are shown. We can notice from this figure that k_1 varies almost linearly, whereas k_3 grows rapidly for larger values of Γ .

The distortion of the free surface is given by

$$\begin{aligned} \eta = & \eta_0 \cos \mathcal{H}\xi \cosh \omega_1 \tau + \eta_0^2 B_{22}(\tau) \cos 2\mathcal{H}\xi \\ & + \eta_0^3 \{B_{31}(\tau) \cos \mathcal{H}\xi + B_{33}(\tau) \cos 3\mathcal{H}\xi\}, \quad (6.1) \end{aligned}$$

where

$$\begin{aligned} \mathcal{H} = & k/k_c, \quad \xi = k_c z, \quad \tau = vt \\ \text{with } & v = 1 + \eta_0^2 v_3, \quad k_c = k_1 + \eta_0^2 k_3. \end{aligned}$$

In addition to the fundamental mode, the presence of various harmonics in (6.1) is the result of the energy transfer from the fundamental mode to the mode of higher orders. The breakup time of the jet is obtained by increasing the time τ in (6.1) until the deepest trough of the wave coincides with the centerline of the planar jet. This is from the fact that the profiles of η corresponding to (3.17)–(3.19) are symmetrical with respect to the z -axis. The breakup time and breakup point was determined by increasing τ and ξ simultaneously in (6.1) until $\eta(\xi, \tau) = -1$ is attained. With the critical value so obtained, (6.1) is used to plot curves of η versus ξ for various values of Γ . We observe that the jet breakup time decreases with increase of the electric field parameter Γ .

In Figs. 3 to 5 we present the profiles of the planar jet. Figs. 4 and 5 show that profiles of η , when K is close to Γ , deviate drastically from those with other values. Also we can notice the the breakup time is relatively short.

- [1] J. W. S. Rayleigh, *Theory of Sound*, Vol. 2., Dover, New York 1947.
- [2] R. J. Donnelly and W. Glaberson, *Proc. Roy. Soc. London* **290A**, 547 (1966).
- [3] M. C. Yuen, *J. Fluid Mech.* **33**, 151 (1968).
- [4] D. P. Wang, *J. Fluid Mech.* **34**, 299 (1968).
- [5] A. H. Nayfeh, *Phys. Fluids* **13**, 841 (1970).
- [6] P. Lafrance, *Phys. Fluids* **18**, 428 (1975)

- [7] A. M. Gañán-Calvo, *J. Fluid Mech.* **335**, 165 (1997).
- [8] A. J. Mestel, *J. Fluid Mech.* **312**, 311 (1996).
- [9] J. R. Melcher, *Field Surface Waves*. M.I.T. Press, Cambridge, Mass. 1963.
- [10] J. M. Crowley, *Phys. Fluids* **8**, 1668 (1965).
- [11] M. Van Dyke, *Perturbation Method in Fluid Mechanics*. Academic Press Inc., New York 1964.